Long-range correlations in disordered metals

C. L. Kane, R. A. Serota, and P. A. Lee
Department of Physics, Massachusetts Institute of Technology, Cambridge, Massachusetts 02139
(Received 30 June 1987)

We address the problem of conductance fluctuations in real space. The nonlocal conductivity tensor and its correlation functions are calculated from the Kubo formula and are shown to exhibit long-ranged behavior. We offer a physical interpretation of our results. The results are used to calculate the long-range spatial correlations in the current density.

I. INTRODUCTION

The phenomenon of sample specific fluctuations in the conductance of small disordered conductors has received much attention in condensed-matter physics. Experimentally[1] and theoretically,[2,3] it has been shown that the conductance of such materials displays reproducable aperiodic fluctuations $\delta G \approx e^2/h$ as a function of magnetic field or chemical potential. Recently, there has been growing interest in effects which arise due to sample geometry. It has been shown that in four-probe conductance measurements the placement of the leads has an important effect,[4] and it has been predicted that the thickness of the leads should affect the average period of the fluctuations, but not their magnitude.[5]

Up to now, theoretical calculations have dealt with the bulk conductance, G, of a rectangular system.[2,3] Such calculations do not contain enough information to account for geometrical effects. In this paper we consider the nonlocal conductivity tensor, $\sigma_{\alpha\beta}(\mathbf{r}_1,\mathbf{r}_2)$. From this quantity one can calculate the current response of a system with any geometry. In addition, one can derive knowledge of local properties, such as the distribution of current density inside of the conductor. We calculate the ensemble averaged quantities

$$\langle \sigma_{\alpha\beta}(\mathbf{r}_1,\mathbf{r}_2)\rangle \quad \text{and} \quad \langle \delta\sigma_{\alpha\beta}(\mathbf{r}_1,\mathbf{r}_2)\delta\sigma_{\gamma\delta}(\mathbf{r}_3,\mathbf{r}_4)\rangle$$

to lowest order in the disorder parameter $(k_F l)^{-1}$, and show that both display long-ranged behavior. The techniques developed here emphasize the role played by current conservation in constraining the form of $\sigma_{\alpha\beta}$.

Our result can be applied to several problems, including spacial correlations in the current density, and current and voltage fluctuations in multilead devices.[6] A similar technique can be used to treat correlations among the transmission amplitudes for different channels and can be applied to the problem of optical transmission.[7]

In Sec. II we examine the conductivity and the constraints imposed by current conservation. We show that the ensemble-averaged conductivity tensor must be a long-ranged object. In Sec. III we exploit current conservation to calculate the second moment of the conductivity tensor. In Sec. IV we offer a physical interpretation of the nonlocal conductivity and the diagrams which represent it. In Sec. V we apply our result to the current-current correlation function and show that it is long ranged, in disagreement with the calculation of Aronov *et al.*[8]

II. THE KUBO FORMULA AND CONDUCTIVITY

The electrical conductivity tensor for a given impurity configuration can be calculated via the Kubo formula, including two spin channels as[9]

$$\sigma_{\alpha\beta}(\mathbf{r},\mathbf{r}') = -(e^2/m^2)\pi[G^+(\mathbf{r}\mathbf{r}') - G^-(\mathbf{r}\mathbf{r}')] \times \overleftrightarrow{\nabla}_\alpha \overleftrightarrow{\nabla}'_\beta [G^+(\mathbf{r}'\mathbf{r}) - G^-(\mathbf{r}'\mathbf{r})] , \tag{2.1}$$

where $\overleftrightarrow{\nabla}_\alpha$ is the antisymmetric gradient operator $\frac{1}{2}(\overrightarrow{\nabla}_\alpha - \overleftarrow{\nabla}_\alpha)$, and G^+ and G^- are advanced and retarded Green's functions for particles at the Fermi surface. As will be shown in Appendix A, when there is time-reversal invariance, the dc conductivity must satisfy

$$\nabla_\alpha \sigma_{\alpha\beta}(\mathbf{r},\mathbf{r}') = \nabla'_\beta \sigma_{\alpha\beta}(\mathbf{r},\mathbf{r}') = 0 . \tag{2.2}$$

The significance of this is that any approximation to the ensemble-averaged conductivity must also satisfy this property. This will greatly simplify the calculation of higher moments.

In addition, this condition allows us to express the current in terms of a classical electric field as follows. The current density can be written as

$$j_\alpha(\mathbf{r}) = \int d\mathbf{r}' \sigma_{\alpha\beta}(\mathbf{r},\mathbf{r}') E_\beta(\mathbf{r}') = \int d\mathbf{r}' \sigma_{\alpha\beta}(\mathbf{r},\mathbf{r}') \nabla'_\beta V(\mathbf{r}') , \tag{2.3}$$

where $E_\beta(\mathbf{r}')$ is the electric field and $V(\mathbf{r}')$ is the electrostatic potential in the sample, which are very complicated and depend on the precise positions of the impurities. We consider a finite sample which is surrounded by insulator and is attached to ideal metallic leads. Due to the divergence condition on $\sigma_{\alpha\beta}(\mathbf{r},\mathbf{r}')$, we can integrate by parts and push the integral to the boundary. Since no current flows out of the insulating boundaries, we know that the normal component of $\sigma_{\alpha\beta}(\mathbf{r},\mathbf{r}')$ must vanish there, so the only contribution comes from the metallic leads. We can then write

$$j_\alpha(\mathbf{r}) = \int_{\text{leads}} d\mathbf{S}'_\beta \sigma_{\alpha\beta}(\mathbf{r},\mathbf{r}') V(\mathbf{r}') . \tag{2.4}$$

Thus we see that due to the constraint on $\sigma_{\alpha\beta}(\mathbf{r},\mathbf{r}')$ the current density depends only on the voltages at the leads, and not on the precise electric field configuration. We can therefore, without loss of generality, write the current density in terms of any potential which has the correct values at the leads. It is convenient to choose the classical potential $V^{\rm cl}(\mathbf{r})$ such that $\nabla^2 V^{\rm cl}(\mathbf{r})=0$ subject to the boundary conditions that $V^{\rm cl}(\mathbf{r})=V(\mathbf{r})$ on the metallic leads and $\nabla_n V(\mathbf{r})=0$ on the insulating boundaries (so that no electric field points outward). In that case we can write

$$j_\alpha(\mathbf{r})=\int d\mathbf{r}'\sigma_{\alpha\beta}(\mathbf{r},\mathbf{r}')E^{\rm cl}_\beta(\mathbf{r}')\ , \tag{2.5}$$

where $E^{\rm cl}_\beta(\mathbf{r}')=\nabla'_\beta V^{\rm cl}(\mathbf{r}')$ is the classical electric field. To calculate the total current we integrate the current density over a cross section. Using a similar technique as above we can get the conductance of a wire as

$$G=\frac{I}{V}=\frac{1}{V^2}\int d\mathbf{r}\,d\mathbf{r}'\sigma_{\alpha\beta}(\mathbf{r},\mathbf{r}')E^{\rm cl}_\alpha(\mathbf{r})E^{\rm cl}_\beta(\mathbf{r}')\ , \tag{2.6}$$

where V is the voltage between the leads.

To illustrate our techniques, we calculate $\langle\sigma_{\alpha\beta}(\mathbf{r},\mathbf{r}')\rangle$. The most important diagrams to lowest order in the disorder are shown in Fig. 1, and their evaluation leads to

$$\begin{aligned}\langle\sigma_{\alpha\beta}(\mathbf{r},\mathbf{r}')\rangle&=\sigma_0[\delta_{\alpha\beta}\bar{\delta}(\mathbf{r}-\mathbf{r}')-\nabla_\alpha\nabla'_\beta d(\mathbf{r},\mathbf{r}')]\\&\equiv\sigma_0\phi_{\alpha\beta}(\mathbf{r},\mathbf{r}')\ ,\end{aligned} \tag{2.7}$$

where $\sigma_0=(e^2/h)(2k_F{}^2l/3\pi)$ is the Boltzman conductivity (in three dimensions). $\bar{\delta}(\mathbf{r}-\mathbf{r}')$ is a sharply peaked function with width l, the mean free path, which can effectively be taken to be a true Dirac δ function. $d(\mathbf{r},\mathbf{r}')$ is the rescaled diffusion propagator which is the sum of the ladder diagram and satisfies the equation

$$-\nabla^2 d(\mathbf{r},\mathbf{r}')=\bar{\delta}(\mathbf{r}-\mathbf{r}')\ , \tag{2.8}$$

subject to the boundary conditions $d(\mathbf{r},\mathbf{r}')=0$ on a conducting boundary and $\nabla_n d(\mathbf{r},\mathbf{r}')=0$ on an insulating boundary.[2] We have also defined the flow function $\phi_{\alpha\beta}(\mathbf{r},\mathbf{r}')$.

This form of the conductivity explicitly satisfies Eq. (2.2). Note the existence of a long-range part $-\sigma_0\nabla_\alpha\nabla'_\beta d(\mathbf{r},\mathbf{r}')$ which results from Fig. 1(b). If we express the conductance in terms of the classical electric field, this long-range part does not enter into the calculation of the conductance. Using Eqs. (2.6) and (2.7), we can write the conductance as

$$\begin{aligned}G=\frac{\sigma_0}{V^2}\Big[&\int d\mathbf{r}[E^{\rm cl}(\mathbf{r})]^2\\&-\int\int d\mathbf{r}\,d\mathbf{r}'\nabla_\alpha\nabla'_\beta d(\mathbf{r},\mathbf{r}')E^{\rm cl}_\alpha(\mathbf{r})E^{\rm cl}_\beta(\mathbf{r}')\Big]\ .\end{aligned} \tag{2.9}$$

Since $\nabla_\alpha E^{\rm cl}_\alpha=0$, the second term can be integrated by parts and pushed to the boundary, and the boundary conditions obeyed by $d(\mathbf{r},\mathbf{r}')$ and $E^{\rm cl}_\alpha(\mathbf{r})$ ensure that this term vanishes. The first term can also be integrated and in the case of a simple wire reduces to the familiar expression

$$G=\sigma_0\frac{A}{L}\ . \tag{2.10}$$

Thus, when the conductance is calculated in this way, the long-range diagram in Fig. 1(b) gives no contribution. For this reason it is convenient to use the classical field when calculating the bulk conductance of a sample with a nontrivial geometry.[5] An alternative way of seeing this is by doing the calculation in momentum space. In that case we are interested in the $q=0$ part of $\langle\sigma(q)\rangle$. Evaluation of diagram 1(a) gives the result (2.10). The current vertices in Fig. 1(b) involve averaging the momentum over the Fermi surface and, therefore, the diagram vanishes. Thus when integrating or equivalently evaluating $\langle\sigma(q=0)\rangle$ one need never worry about the long-range diagram. One cannot, however, ignore it in the calculation of $\langle\sigma_{\alpha\beta}(\mathbf{r}_1,\mathbf{r}_2)\rangle$.

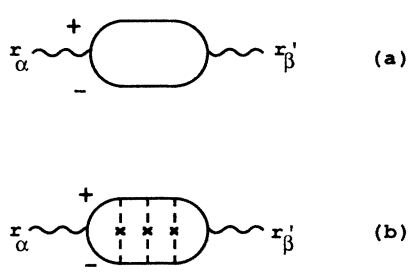

FIG. 1. Diagrams contributing to $\langle\sigma_{\alpha\beta}(\mathbf{r}_1,\mathbf{r}_2)\rangle$. (a) is the short-range part and (b) is the long-range part.

III. CORRELATION FUNCTION OF THE CONDUCTIVITY

Calculation of

$$C_{\alpha\beta\gamma\delta}(\mathbf{r}_1,\mathbf{r}_2;\mathbf{r}_3,\mathbf{r}_4)\equiv\langle\delta\sigma_{\alpha\beta}(\mathbf{r}_1,\mathbf{r}_2)\delta\sigma_{\gamma\delta}(\mathbf{r}_3,\mathbf{r}_4)\rangle$$

involves drawing two conductivity bubble diagrams and dressing them with impurity lines in all possible ways such that the bubbles are connected. This procedure is similar to the calculation of conductance fluctuations,[2,3] except for the following complication. In the case of conductance fluctuations the external current vertices are integrated over all space. Therefore, these vertices can be evaluated in the momentum representation, and it is well known that all impurity lines which dress a single current vertex as a vertex correction vanish upon momentum integration. Consequently, the diagrams can be enumerated in a rather straightforward manner.[2,3] However, in the present problem, we do not integrate over the external position, and these vertex corrections must be kept as they were in the calculation of the conductivity. Thus, the number of diagrams proliferates. The problem is even worse, however, in that even after enumerating all of the diagrams it is not possible to evaluate them in a straightforward way because individual diagrams contain spurious divergencies which are difficult to handle. These

difficulties are discussed in Appendix B.

It is possible to avoid this problem by exploiting the constraint that current conservation imposes on this quantity. The details of this calculation will be presented in Appendix B. The end result is that we can account for the long-range nature of the current vertices by convolving each bare vertex with a flow function $\phi_{\alpha\alpha'}(\mathbf{r},\mathbf{r}')$. That is, we can write

$$C_{\alpha\beta\gamma\delta}(\mathbf{r}_1,\mathbf{r}_2;\mathbf{r}_3,\mathbf{r}_4)=\int\int\int\int d\mathbf{r}_1'd\mathbf{r}_2'd\mathbf{r}_3'd\mathbf{r}_4'\phi_{\alpha\alpha'}(\mathbf{r}_1,\mathbf{r}_1')\phi_{\beta\beta'}(\mathbf{r}_2,\mathbf{r}_2')\phi_{\gamma\gamma'}(\mathbf{r}_3,\mathbf{r}_3')\phi_{\delta\delta'}(\mathbf{r}_4,\mathbf{r}_4')\Gamma_{\alpha'\beta'\gamma'\delta'}(\mathbf{r}_1',\mathbf{r}_2';\mathbf{r}_3',\mathbf{r}_4'), \tag{3.1}$$

where now $\Gamma_{\alpha\beta\gamma\delta}(\mathbf{r}_1,\mathbf{r}_2;\mathbf{r}_3,\mathbf{r}_4)$ are the diagrams where the impurity dressings of a single external current vertex are omitted. As shown in Fig. 2, these are the same as the two-, three-, and four-diffusion-propagator diagrams introduced by Lee and Stone,[2] except that the external vertices are not integrated over. Note that equation (3.1) explicitly satisfies current conservation since $\nabla_\alpha\phi_{\alpha\beta}(\mathbf{r},\mathbf{r}')=0$.

The quantity $\langle\delta G^2\rangle$ can be calculated for a wire by integrating $C_{\alpha\beta\gamma\delta}(\mathbf{r}_1,\mathbf{r}_2;\mathbf{r}_3,\mathbf{r}_4)$ over all of its variables against the uniform classical electric field $E_z^{\rm cl}$. As in the case of $\langle\sigma_{\alpha\beta}(\mathbf{r}_1,\mathbf{r}_2)\rangle$, the long-range part of $\phi_{\alpha\beta}$ gives no contribution when integrated, so our result reduces to

$$\langle\delta G^2\rangle=\frac{1}{L^4}\int\int\int\int d\mathbf{r}_1d\mathbf{r}_2d\mathbf{r}_3d\mathbf{r}_4\Gamma_{zzzz}(\mathbf{r}_1,\mathbf{r}_2;\mathbf{r}_3,\mathbf{r}_4), \tag{3.2}$$

which is precisely the result of Lee and Stone.

Contrary to what was stated in Ref. 2, diagrams 2(d) and 2(e) do not cancel, and a correct evaluation of $\Gamma_{\alpha\beta\gamma\delta}(\mathbf{r}_1,\mathbf{r}_2;\mathbf{r}_3,\mathbf{r}_4)$ must include both of them. However, upon integration over $\mathbf{r}_1,\ldots,\mathbf{r}_4$, these diagrams do cancel and the final result for $\langle\delta G^2\rangle$ is correctly given in Ref. 2. In fact, as will be shown in Appendix C, when integrated over a cross section, all of the diagrams with no change in the sign of the energy at a current vertex cancel. In that case, as stated by Alt'shuler *et al.*,[3] it is possible to express our result in terms of Γ^{+-}, which consists only of the diagrams with two diffusion propagators and no change in the sign of the energy at the current vertices shown in Fig. 3. These diagrams can easily be evaluated as

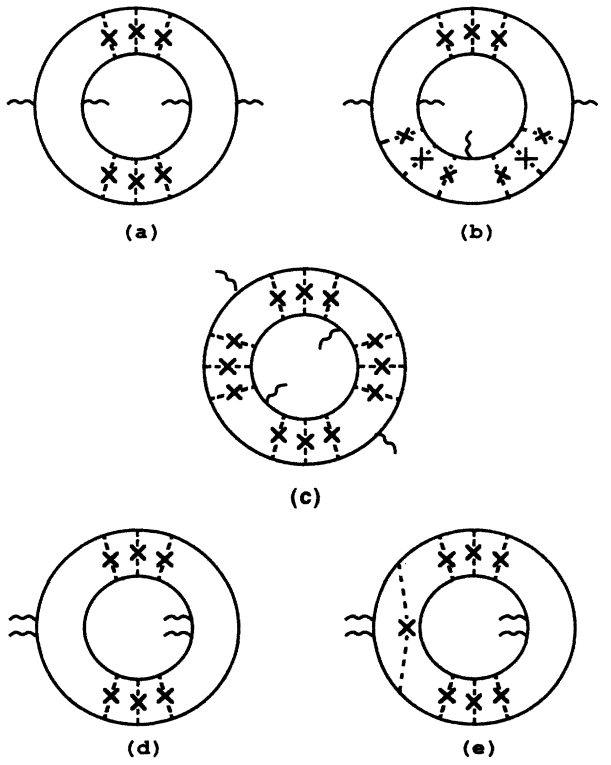

FIG. 2. Two-, three-, and four-diffusion-propagator diagrams contributing to $\Gamma_{\alpha\beta\gamma\delta}(\mathbf{r}_1,\mathbf{r}_2;\mathbf{r}_3,\mathbf{r}_4)$. The current vertices are represented by the wavy lines and can be labeled $\mathbf{r}_1$, $\mathbf{r}_2$, $\mathbf{r}_3$, and $\mathbf{r}_4$ in all possible ways. These are the same as the diagrams presented by Lee and Stone (Ref. 2).

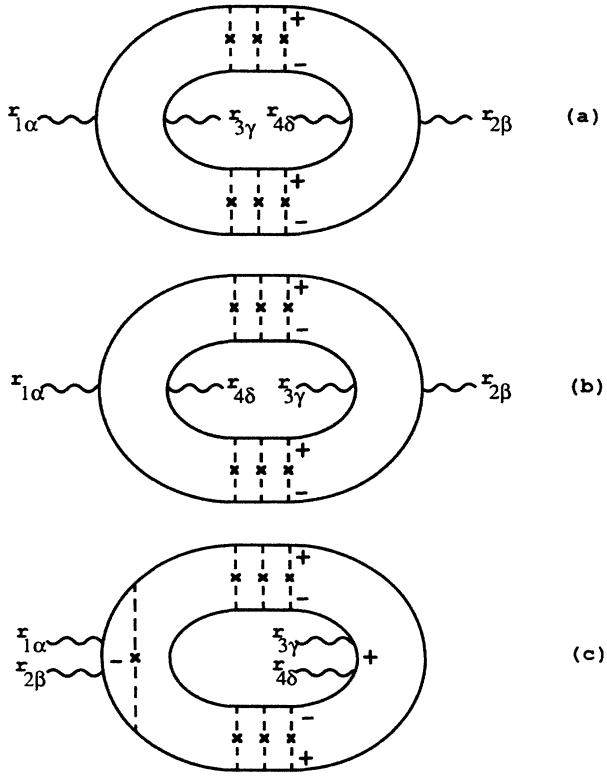

FIG. 3. Two-diffusion-propagator diagrams contributing to $\Gamma^{+-}_{\alpha\beta\gamma\delta}(\mathbf{r}_1,\mathbf{r}_2;\mathbf{r}_3,\mathbf{r}_4)$.

$$\Gamma^{+-}_{\alpha\beta\gamma\delta}(\mathbf{r}_1,\mathbf{r}_2;\mathbf{r}_3,\mathbf{r}_4)=16\left[\frac{e^2}{h}\right]^2[\delta_{\alpha\gamma}\delta_{\beta\delta}\delta(\mathbf{r}_1-\mathbf{r}_3)\delta(\mathbf{r}_2-\mathbf{r}_4)d(\mathbf{r}_1,\mathbf{r}_2)^2+\delta_{\alpha\delta}\delta_{\beta\gamma}\delta(\mathbf{r}_1-\mathbf{r}_4)\delta(\mathbf{r}_2-\mathbf{r}_3)d(\mathbf{r}_1,\mathbf{r}_2)^2$$

$$+\delta_{\alpha\beta}\delta_{\gamma\delta}\delta(\mathbf{r}_1-\mathbf{r}_2)\delta(\mathbf{r}_3-\mathbf{r}_4)d(\mathbf{r}_1,\mathbf{r}_2)^2]\ . \tag{3.3}$$

The first two terms in this sum correspond to Figs. 3(a) and 3(b). The third term is the sum of diagrams similar to Fig. 3(c). Each segment containing the two current vertices may or may not include the extra impurity dressing. This dressing is similar to that encountered in Hikami vertices;[10] however, there is no complete cancelation. The sum of the bare vertex and the dressed vertex turns out to have a value of half the bare vertex. Therefore, if we include all possibilities of the two vertices being dressed or bare (four terms), the total value would be $\frac{1}{4}$ of the value of the completely bare diagram. An additional factor of 4 arises, however, because we can interchange $\mathbf{r}_1$ and $\mathbf{r}_2$ or $\mathbf{r}_3$ and $\mathbf{r}_4$. Therefore, the sum of all of these diagrams represented by Fig. 3(c) contribute the same numerical value as the single diagrams shown in Figs. 3(a) and 3(b) (which cannot be dressed). In Eq. (3.3) we have also included both particle-particle and particle-hole channels. If one plugs this expression into (3.2), then one gets $\langle\delta G^2\rangle\approx(e^2/h)^2$ with the exact numerical coefficients as those predicted by Lee and Stone.[2]

It is possible to include inelastic effects into these calculations. By particle conservation, the diffusion propagators dressing the current vertices cannot be altered by inelastic scattering. Therefore $\phi_{\alpha\beta}(\mathbf{r},\mathbf{r}')$ is unchanged. As shown in Ref. 2, the diffusion propagators contained in Γ are ladder diagrams between Green's functions describing different measurements. They are therefore connected only by impurity lines and not interaction lines, so the usual cancellation between self-energy and vertex corrections does not occur.[2] The inelastic effects can be included by inserting an inelastic length into the diffusion equation obeyed by the propagators in Γ:

$$(-\nabla^2+L_{\text{in}}^{-2})d(\mathbf{r},\mathbf{r}')=\delta(\mathbf{r}-\mathbf{r}')\ . \tag{3.4}$$

IV. PHYSICAL INTERPRETATION

There are two different ways of interpreting the quantity $\sigma_{\alpha\beta}(\mathbf{r},\mathbf{r}')$. The standard way is to think of it as the current response at $\mathbf{r}$ due to an electric field at $\mathbf{r}'$. This is the view we will take when we calculate the current-current correlation function. One can obtain more physical insight into the quantities

$$\langle\sigma_{\alpha\beta}(\mathbf{r}_1,\mathbf{r}_2)\rangle \quad\text{and}\quad \langle\sigma_{\alpha\beta}(\mathbf{r}_1,\mathbf{r}_2)\sigma_{\gamma\delta}(\mathbf{r}_3,\mathbf{r}_4)\rangle$$

and the diagrams which represent them by considering $\sigma_{\alpha\beta}(\mathbf{r}_1,\mathbf{r}_2)$ as a kind of transmission amplitude. To see how this works, note that the total current going through a wire can be written as

$$I=\int\int d\mathbf{S}_\alpha d\mathbf{r}'\sigma_{\alpha\beta}(\mathbf{r},\mathbf{r}')E_\beta(\mathbf{r}')\ , \tag{4.1}$$

where the integral over $d\mathbf{S}_\alpha$ is taken over any cross section. If we use the facts that $E_\alpha=\nabla_\alpha V$ and $\nabla_\alpha\sigma_{\alpha\beta}=0$, we can apply the divergence theorem to the $\mathbf{r}'$ integral and push it to the surface. Since no current flows out of the insulating boundaries, we know that there will only be a contribution at the leads. We can choose V to be zero on one of the leads, so we obtain

$$G=\frac{I}{V}=\int\int d\mathbf{S}_\alpha d\mathbf{S}'_\beta\sigma_{\alpha\beta}(\mathbf{r},\mathbf{r}')\ , \tag{4.2}$$

where V is the voltage between the leads. Because of the divergence condition on σ, the integrals over $d\mathbf{S}$ and $d\mathbf{S}'$ can be taken over any cross section; however, if we choose them to be at opposite leads, then we can consider (4.2) to be a real-space version of the relation

$$G=\frac{e^2}{h}\sum_{a,b}T_{ab}\ , \tag{4.3}$$

where T_{ab} is the transmission amplitude between transverse momentum channel a and b at opposite leads.[9] That is, $\sigma_{\alpha\beta}(\mathbf{r},\mathbf{r}')$ is a real-space transmission amplitude. This sort of analysis can easily be generalized to the case of multilead geometries, in which the current going through each lead can be expressed in terms of the voltage at each lead via

$$I_i=\sum_j G_{ij}V_j\ , \tag{4.4}$$

where i and j label the leads, and

$$G_{ij}\equiv\int\int d\mathbf{S}_{i\alpha}d\mathbf{S}'_{j\beta}\sigma_{\alpha\beta}(\mathbf{r},\mathbf{r}') \tag{4.5}$$

is the generalized conductance tensor for a multilead device.

With this in mind, we now attempt to physically motivate the diagrams which contribute to the averaged conductivity and its correlation function. The arguments presented here are based on Feynman's idea of summing over paths, and are not meant to be rigorous, but are rather a guide for the intuition.

The transmission amplitude $\sigma_{\alpha\beta}(\mathbf{r},\mathbf{r}')$ will be related to the square of the sum over all Feynman paths of the amplitude to get from $\mathbf{r}$ to $\mathbf{r}'$. If we assume that $\mathbf{r}$ and $\mathbf{r}'$ are separated by more than a mean free path, then the electrons must be scattered by impurities, and the different paths that the electron can take can be characterized by the impurities which they visit. If on a particular path the electron visits impurities at $\mathbf{r}_1,\mathbf{r}_2,\ldots,\mathbf{r}_N$, then the Feynman amplitude for that path will be proportional to

$$A^+(\mathbf{r},\mathbf{r}')$$
$$\propto G^+(\mathbf{r},\mathbf{r}_1)G^+(\mathbf{r}_1,\mathbf{r}_2)\cdots G^+(\mathbf{r}_{N-1},\mathbf{r}_N)G^+(\mathbf{r}_N,\mathbf{r}')\ . \tag{4.6}$$

The total probability will then be

$$P(\mathbf{r},\mathbf{r}') \propto \left| \sum_{\text{path } i} A_i^+(\mathbf{r},\mathbf{r}') \right|^2 = \sum_{i,j} A_i^+(\mathbf{r},\mathbf{r}') A_j^-(\mathbf{r},\mathbf{r}') , \quad (4.7)$$

where we have defined $A_i^- = (A_i^+)^*$. It is convenient to think of this as an amplitude for a particle (A^+) and a hole (A^-) to propagate from $\mathbf{r}$ to $\mathbf{r}'$. This interpretation is not meant to be taken literally; it is just a convenient way of thinking of the two terms in the square.

The ladder diagram in Fig. 1(b) corresponds to the diagonal terms in the expansion:

$$D(\mathbf{r},\mathbf{r}') \propto \sum_i A_i^+(\mathbf{r},\mathbf{r}') A_i^-(\mathbf{r},\mathbf{r}') . \quad (4.8)$$

In the particle-hole picture, the particle and the hole visit the same impurities when going from $\mathbf{r}$ to $\mathbf{r}'$. Typically, the phase of A_i oscillates rapidly modulo 2π and is essentially $k_F L_i$ (where L_i is the total path length). This phase dependence cancels out in Eq. (4.8). D is therefore the sum over all possible random walks of a real quantity, and represents the classical diffusion process when the mean free path is much smaller than the sample size. To account for the current nature of $\sigma_{\alpha\beta}$, one must include gradients

$$\sigma_{\alpha\beta}(\mathbf{r},\mathbf{r}') \propto \nabla_\alpha \nabla'_\beta D(\mathbf{r},\mathbf{r}') . \quad (4.9)$$

The δ-function term in Eq. (2.7) is absent because $\mathbf{r}$ and $\mathbf{r}'$ are separated by more than a mean free path. If we allow $\mathbf{r}$ and $\mathbf{r}'$ to be near each other, then the electrons could propagate without scattering. This process is represented in Fig. 1(a) and contributes the δ function.

In general, there will be interference terms (cross terms) in Eq. (4.7). If we ignore weak localization effects (which can be understood with similar arguments), then upon ensemble averaging over all impurity positions, the rapid phase dependence of these terms will make them average to zero. If we do not average, then it is these interference terms which are responsible for the sample-dependent fluctuations in σ and, hence, universal conductance fluctuations.

To investigate fluctuations we look at the product of two σ's: $\langle \sigma_{\alpha\beta}(\mathbf{r}_1,\mathbf{r}_2)\sigma_{\gamma\delta}(\mathbf{r}_3,\mathbf{r}_4)\rangle$. This is related to the probability for two electrons to go from $\mathbf{r}_1$ to $\mathbf{r}_2$ and $\mathbf{r}_3$ to $\mathbf{r}_4$:

$$P(\mathbf{r}_1,\mathbf{r}_2)P(\mathbf{r}_3,\mathbf{r}_4) \propto \sum_{i,j,k,l} A_i^+(\mathbf{r}_1,\mathbf{r}_2) A_j^-(\mathbf{r}_1,\mathbf{r}_2) \times A_k^+(\mathbf{r}_3,\mathbf{r}_4) A_l^-(\mathbf{r}_3,\mathbf{r}_4) . \quad (4.10)$$

Alternatively, we can view this as an amplitude for the propagation of two particle-hole pairs. To obtain the fluctuations, we subtract the product of the averages (the diagonal terms with $i=j$ and $k=l$) and ensemble average. What remains are those combinations of paths for which the rapid phase dependence cancels out. This can occur if the electron-hole pairs "switch partners," as shown in Fig. 4. Such a process is represented in Fig. 4(a). The thick lines represent the particles and the thin lines represent the holes. The particle-hole pairs propagate to an intermediate point where they "switch partners." They then propagate and switch back. In Fig. 4(b) we show a schematic Feynman diagram which would represent this process. It can be recognized as the two-diffusion-propagator diagram shown in Fig. 2(a) with all of the current vertices dressed with diffusion ladders. We could alternatively have processes where some or all of the vertices were bare. In that case the particle-hole pairs would switch immediately after entering the sample. All of these processes are included in Eq. (3.1). It is through these processes that quantum interference manifests itself in the correlation function of the conductivity.

V. THE CURRENT-CURRENT CORRELATION FUNCTION

We will now apply the result (3.1) to the calculation of the current-current correlation function. For simplicity we consider a translationally invariant system in which the diffusion propagator in three dimensions is

$$d(\mathbf{r},\mathbf{r}') = 1/(4\pi |\mathbf{r}-\mathbf{r}'|) . \quad (5.1)$$

If we consider a uniform classical electric field $E^{\text{cl}} = E$ in the z direction, then the current density is

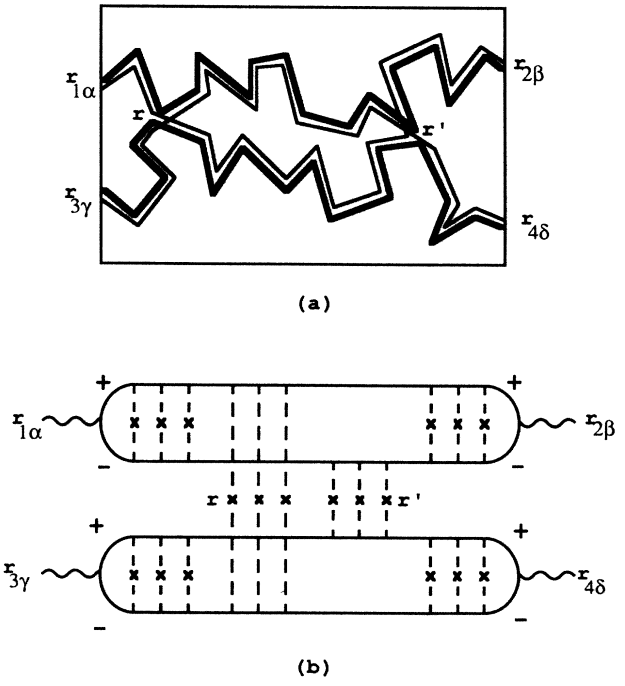

FIG. 4. (a) A real-space picture of the interfering paths which contribute to $\langle \delta\sigma_{\alpha\beta}(\mathbf{r}_1,\mathbf{r}_2)\delta\sigma_{\gamma\delta}(\mathbf{r}_3,\mathbf{r}_4)\rangle$. The thick line represents the particle and the thin line represents the hole. (b) A schematic drawing of the Feynman diagram which represents the process shown in (a).

$$j_\alpha(\mathbf{r}) = E \int d\mathbf{r}' \sigma_{\alpha z}(\mathbf{r},\mathbf{r}') \ . \tag{5.2}$$

The current-current correlation function can then be written as

$$\langle j_\alpha(\mathbf{r}_1) j_\beta(\mathbf{r}_2)\rangle = E^2 \int\int d\mathbf{r}_3 d\mathbf{r}_4 C_{\alpha z \beta z}(\mathbf{r}_1,\mathbf{r}_3;\mathbf{r}_2,\mathbf{r}_4) \ . \tag{5.3}$$

The long-range part of $\phi_{\alpha\beta}$ vanishes when it is integrated, so we can write

$$\langle \delta j_\alpha(\mathbf{r}_1)\delta j_\beta(\mathbf{r}_2)\rangle = E^2 \int\int\int\int d\mathbf{r}_1' d\mathbf{r}_2' d\mathbf{r}_3 d\mathbf{r}_4 \phi_{\alpha\alpha'}(\mathbf{r}_1,\mathbf{r}_1')\phi_{\beta\beta'}(\mathbf{r}_2,\mathbf{r}_2')\Gamma_{\alpha' z \beta' z}(\mathbf{r}_1';\mathbf{r}_3;\mathbf{r}_2';\mathbf{r}_4) \ . \tag{5.4}$$

In principle, one must evaluate all of the diagrams contained in Γ, including three and four diffusion propagators, since we are not integrating over the cross section; however, we can show that the dominant contribution comes from the diagrams shown in Fig. 3(c) and a similar three-diffusion-propagator diagram in which the $\mathbf{r}_1$ and $\mathbf{r}_2$ vertices are next to each other, as in 3(c). Evaluation of the diagram in Fig. 3(c) yields

$$4\left[\frac{e^2}{h}\right]^2 \int d\mathbf{r}_1' \phi_{\alpha\alpha'}(\mathbf{r}_1,\mathbf{r}_1')\phi_{\beta\alpha'}(\mathbf{r}_2,\mathbf{r}_1') \int d\mathbf{r}_3 [d(\mathbf{r}_1',\mathbf{r}_3)]^2 \ . \tag{5.5}$$

We can separate the integrals because of translational invariance, and if we use the fact that

$$\int d\mathbf{r}\, \phi_{\alpha\alpha'}(\mathbf{r}_1,\mathbf{r})\phi_{\beta\alpha'}(\mathbf{r}_2,\mathbf{r}) = \phi_{\alpha\beta}(\mathbf{r}_1,\mathbf{r}_2) \ , \tag{5.6}$$

we get

$$\langle \delta j_\alpha(\mathbf{r}_1)\delta j_\beta(\mathbf{r}_2)\rangle \propto E^2 \phi_{\alpha\beta}(\mathbf{r}_1,\mathbf{r}_2) L \ , \tag{5.7}$$

where we have cut off the integral by the sample size L. This term shows long-range behavior; it is essentially proportional to L/R^3 in three dimensions, where $\mathbf{R}=\mathbf{r}_1-\mathbf{r}_2$ and $R = |\mathbf{R}|$. The three-diffusion-propagator diagram gives a similar result, and it can be shown that all of the other diagrams give contributions which are equal to or less than $R^{-2}\ln L/R$. The total result for $R < L$ is then

$$\langle \delta j_\alpha(\mathbf{r}_1)\delta j_\beta(\mathbf{r}_2)\rangle = \begin{cases} (e^2/h)^2 E^2 L(\delta_{\alpha\beta} - \mathbf{R}_\alpha \mathbf{R}_\beta)/R^3 & \text{in three dimensions} \ , \\ (e^2/h)^2 E^2 L^2(\delta_{\alpha\beta} - \mathbf{R}_\alpha \mathbf{R}_\beta)/R^2 & \text{in two dimensions} \ . \end{cases} \tag{5.8}$$

This result disagrees with the short-range correlation function calculated by Aronov *et al.*[8] because they did not include the long-range nature of the dressed current vertex. The long-range current correlations are unfortunately difficult to observe. One can calculate the fluctuation in the magnetic field generated by the fluctuating currents; however, as will be shown in Appendix D, the long-range correlations do not affect them, and the results quoted by Aronov *et al.*[8] remain valid.

VI. CONCLUSION

To calculate the effects of sample geometry on conductance measurements, it is necessary to know the nonlocal conductivity tensor. The techniques developed here provide a means of calculating the ensemble-averaged quantities

$$\langle \sigma_{\alpha\beta}(\mathbf{r}_1,\mathbf{r}_2)\rangle \quad \text{and} \quad \langle \delta\sigma_{\alpha\beta}(\mathbf{r}_1,\mathbf{r}_2)\delta\sigma_{\gamma\delta}(\mathbf{r}_3,\mathbf{r}_4)\rangle$$

via Eqs. (2.7) and (3.1). The only input to these calculations is the diffusion propagator $d(\mathbf{r},\mathbf{r}')$, which is the Green's function for the classical diffusion equation subject to the boundary conditions appropriate to the sample. This reflects the fact that diffusion is the physical process which determines both of these quantities. $\langle \sigma_{\alpha\beta}(\mathbf{r}_1,\mathbf{r}_2)\rangle$ is essentially an amplitude for an electron to classically diffuse from $\mathbf{r}_1$ to $\mathbf{r}_2$, while

$$\langle \delta\sigma_{\alpha\beta}(\mathbf{r}_1,\mathbf{r}_2)\delta\sigma_{\gamma\delta}(\mathbf{r}_3,\mathbf{r}_4)\rangle$$

is an amplitude for two electrons to interfere diffusively, as explained in Sec. IV.

The result (3.1) can be applied to the problem of voltage fluctuations in multilead devices. By inverting the generalized conductance tensor defined in (4.4) and (4.5), one can calculate the voltages at each lead. We can then apply this technique to calculate their fluctuations.[6] We can also calculate correlations in the transmission amplitudes defined by Fisher and Lee.[9] In light of the similarity between the nonlocal conductivity tensor and the transmission amplitude, the only difference in these calculations is that we must define "channel" current vertices which involve Fourier-transformed Green's functions.[7] Lastly, as we have shown, the current-current correlation function can be calculated and exhibits an interesting long-range behavior.

ACKNOWLEDGMENTS

We would like to thank D. DiVincenzo and S. Maekawa for useful discussions. This work was supported by the National Science Foundation under Grant No. DMR-85-21377.

APPENDIX A

In this appendix we examine the consequences that current conservation has on the quantity $\sigma_{\alpha\beta}(\mathbf{r},\mathbf{r}')$. The dc conductivity can be expressed in terms of the electromagnetic response kernel $K_{\alpha\beta}(\mathbf{r},\mathbf{r}')$ as

$$\sigma_{\alpha\beta}(\mathbf{r},\mathbf{r}')=\lim_{\omega\to 0}\frac{1}{i\omega}K_{\alpha\beta}(\mathbf{r},\mathbf{r}',\omega)\ , \tag{A1}$$

where $K_{\alpha\beta}(\mathbf{r},\mathbf{r}',\omega)$ is the current response to an externally applied vector potential. Since we are concerned with the real part of σ, we need only concern ourselves with the imaginary part of $K_{\alpha\beta}$, so we can ignore the diamagnetic term. We can expand $K_{\alpha\beta}$ in a spectral representation:

$$\mathrm{Im}K_{\alpha\beta}(\mathbf{r},\mathbf{r}')=\mathrm{Im}\sum_N\frac{\langle 0\,|\,j_\alpha(\mathbf{r})\,|\,N\rangle\langle N\,|\,j_\beta(\mathbf{r}')\,|\,0\rangle}{\omega-\omega_{N0}+i\eta}-\frac{\langle 0\,|\,j_\beta(\mathbf{r}')\,|\,N\rangle\langle N\,|\,j_\alpha(\mathbf{r})\,|\,0\rangle}{\omega+\omega_{N0}+i\eta}\ , \tag{A2}$$

where $\omega_{N0}=E_N-E_0$ and $j_\alpha(\mathbf{r})$ is the second-quantized current operator. If we take the divergence of this quantity, then current conservation requires that $\nabla_\alpha j_\alpha(\mathbf{r})+i\omega\rho(\mathbf{r})=0$, where $\rho(\mathbf{r})$ is the density operator. We can then write the divergence of the conductance as

$$\begin{aligned}\mathrm{Re}\nabla_\alpha\sigma_{\alpha\beta}(\mathbf{r},\mathbf{r}')&=\lim_{\omega\to 0}\mathrm{Re}\sum_N\frac{\langle 0\,|\,\rho(\mathbf{r})\,|\,N\rangle\langle N\,|\,j_\beta(\mathbf{r}')\,|\,0\rangle}{\omega-\omega_{N0}+i\eta}-\frac{\langle 0\,|\,j_\beta(\mathbf{r}')\,|\,N\rangle\langle N\,|\,\rho(\mathbf{r})\,|\,0\rangle}{\omega+\omega_{N0}+i\eta}\\&=2\,\mathrm{Re}\sum_N\frac{\langle 0\,|\,\rho(\mathbf{r})\,|\,N\rangle\langle N\,|\,j_\beta(\mathbf{r}')\,|\,0\rangle}{-\omega_{N0}}\ .\end{aligned} \tag{A3}$$

We can ignore $i\eta$ because there is no contribution for the $N=0$ term. If there is time-reversal invariance, then we can choose the wave functions to be real. Matrix elements of the density operator will be real, while matrix elements of the current operator will be imaginary. The divergence therefore vanishes when there is time-reversal invariance. This procedure can be repeated on $\mathbf{r}'$, so we get

$$\nabla_\alpha\sigma_{\alpha\beta}(\mathbf{r},\mathbf{r}')=\nabla'_\beta\sigma_{\alpha\beta}(\mathbf{r},\mathbf{r}')=0\ . \tag{A4}$$

These arguments are not valid in the presence of a magnetic field which breaks time-reversal symmetry.

Alternatively, one can show this directly from the Kubo formula (1). Upon taking the divergence, one finds

$$\nabla_\alpha\sigma_{\alpha\beta}(\mathbf{r},\mathbf{r}')\propto\nabla^2(G^+-G^-)\overleftrightarrow{\nabla}'_\beta(G^+-G^-)-(G^+-G^-)\overleftrightarrow{\nabla}'_\beta\nabla^2(G^+-G^-)\ . \tag{A5}$$

The unaveraged Green's function for electrons at the Fermi level in the absence of a magnetic field satisfies the equation of motion

$$\left[\frac{\nabla^2}{2m}+\mu\right]G^\pm(\mathbf{r},\mathbf{r}')=\delta(\mathbf{r}-\mathbf{r}')+V(\mathbf{r})G^\pm(\mathbf{r},\mathbf{r}')\ , \tag{A6}$$

where $V(\mathbf{r})$ is the impurity potential. Therefore,

$$\nabla^2[G^+(\mathbf{r},\mathbf{r}')-G^-(\mathbf{r},\mathbf{r}')]=2m[V(\mathbf{r})-\mu][G^+(\mathbf{r},\mathbf{r}')-G^-(\mathbf{r},\mathbf{r}')]\ . \tag{A7}$$

All of the terms therefore cancel and the divergence is zero.

APPENDIX B

To calculate $C_{\alpha\beta\gamma\delta}$, one must, in principle, write down all of the diagrams and evaluate them all. There are many diagrams which contribute in addition to the diagrams given by Lee and Stone. A few of them are shown in Fig. 5. The square and hexagonal vertices must be dressed by impurity lines to form Hikami vertices.[10] Evaluation of these diagrams leads to spurious divergencies. To illustrate this, consider the diagram in Fig. 5(a) evaluated in momentum space. Each Hikami vertex gives a contribution[10]

$$H(\mathbf{q}_1,\mathbf{q}_2,\mathbf{q}_3,\mathbf{q}_4)=(D\tau^3/u^2)\delta(\mathbf{q}_1+\mathbf{q}_2+\mathbf{q}_3+\mathbf{q}_4)\times(\mathbf{q}_1^2+\mathbf{q}_3^2-2\mathbf{q}_2\cdot\mathbf{q}_4)\ . \tag{B1}$$

Each ladder diagram (diffusion propagator) is

$$D(\mathbf{q})=u^2/(D\tau\mathbf{q}^2)\ . \tag{B2}$$

The segments connected to the current vertices give a contribution

$$V_\alpha(\mathbf{q})=[2D/(u^2\tau)]iq_\alpha\ . \tag{B3}$$

The entire diagram can then be written as

$$16\frac{q_{1\alpha}q_{2\beta}q_{3\gamma}q_{4\delta}}{\mathbf{q}_1^2\mathbf{q}_2^2\mathbf{q}_3^2\mathbf{q}_4^2}\sum_{\mathbf{q},\mathbf{q}'}\frac{1}{\mathbf{q}^2}\frac{1}{\mathbf{q}'^2}(\mathbf{q}^2+\mathbf{q}'^2-2\mathbf{q}_1\cdot\mathbf{q}_3)(\mathbf{q}^2+\mathbf{q}'^2-2\mathbf{q}_2\cdot\mathbf{q}_4)\delta(\mathbf{q}+\mathbf{q}'+\mathbf{q}_1+\mathbf{q}_3)\delta(\mathbf{q}+\mathbf{q}'+\mathbf{q}_2+\mathbf{q}_4)\ . \tag{B4}$$

If we consider small external momentum, then $\mathbf{q}=\mathbf{q}'$, and there will be a term which is proportional to

$$\sum_{\mathbf{q}}1\ . \tag{B5}$$

This sum must have an upper cutoff. However, to evaluate it, one must be able to describe the physics on length scales smaller than the mean free path. This is clearly beyond the scope of the diffusion approximation. One could repeat this exercise in real space and the divergences would manifest themselves as δ functions evaluated at zero. The other diagrams in Fig. 5 contain similar divergencies or are spurious and must be canceled. For example, Fig. 5(c) is nominally canceled by a diagram where the single impurity line connects the $+-$ lines instead of the $++$ lines as shown. However, it is not legitimate to stop at a single impurity connecting $+$ and $-$ lines without summing the full ladder, and the resulting diagram [which is contained in the hexagonal diagram 5(b)] again contains spurious divergences. On physical

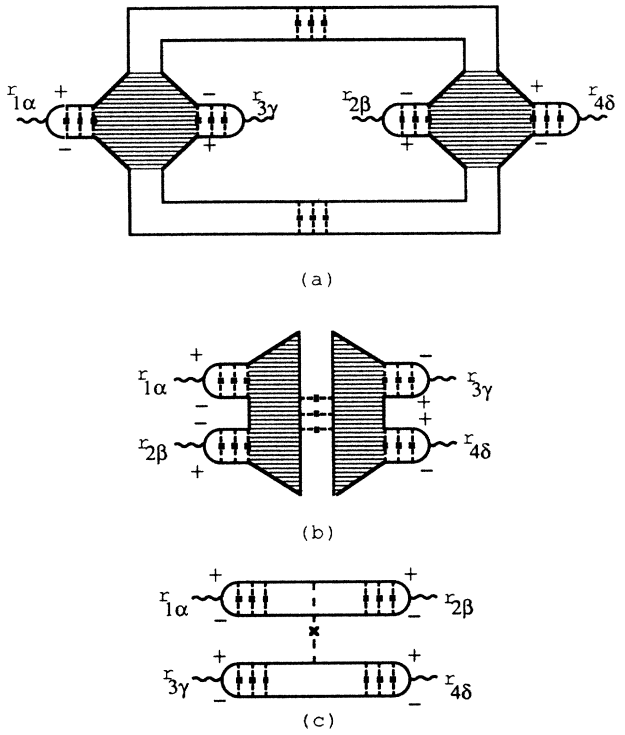

FIG. 5. A few of the diagrams which one could write down for $\langle \delta\sigma_{\alpha\beta}(\mathbf{r}_1,\mathbf{r}_2)\delta\sigma_{\gamma\delta}(\mathbf{r}_3,\mathbf{r}_4)\rangle$. The shaded diamonds in (a) and hexagons in (b) are the dressed Hikami vertices (Ref. 10).

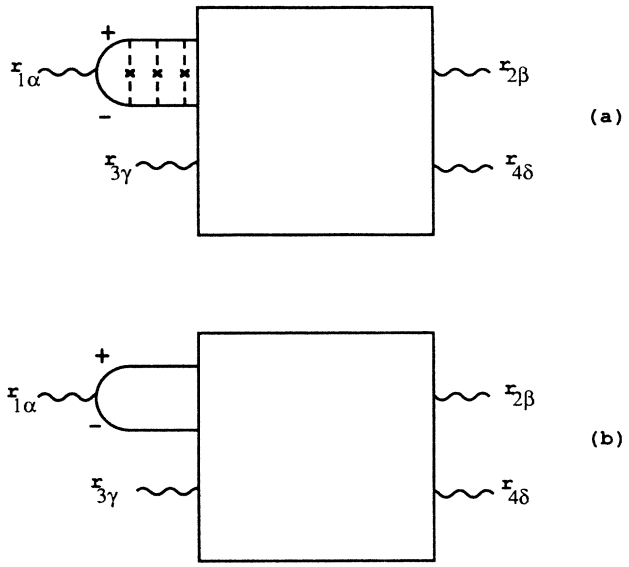

FIG. 6. Division of diagrams for $\langle \delta\sigma_{\alpha\beta}(\mathbf{r}_1,\mathbf{r}_2)\delta\sigma_{\gamma\delta}(\mathbf{r}_3,\mathbf{r}_4)\rangle$ into (a) those with a diffusion ladder dressing the $\mathbf{r}_1$ vertex, and (b) everything else.

grounds, one would expect that when all of the diagrams are accounted for, these divergencies would cancel out. It is difficult, however, to show this with brute-force evaluation.

It is possible to circumvent this problem by imposing the constraint that current conservation holds on $C_{\alpha\beta\gamma\delta}$—it must be divergenceless on all four of its variables. To illustrate this technique, it is convenient to look at $C_{\alpha\beta\gamma\delta}(\mathbf{r}_1,\mathbf{r}_2;\mathbf{r}_3,\mathbf{r}_4)$ as a function of one of its variables, ignoring the dependence of the others for the moment. As shown in Fig. 6, we can divide the diagrams for $C_\alpha(\mathbf{r}_1)$ into two classes: (1) those diagrams which have the $\mathbf{r}_1$ current vertex dressed by a diffusion ladder, and (2) everything else. The diagrams in class 1 all consist of the gradient of a diffusion propagator convolved against some function, so we can define $\Lambda(\mathbf{r}_1)$ and $\Gamma_\alpha(\mathbf{r}_1)$ such that

$$C_\alpha(\mathbf{r}_1)=\int d\mathbf{r}_1'\nabla_{1\alpha}d(\mathbf{r}_1,\mathbf{r}_1')\Lambda(\mathbf{r}_1')+\Gamma_\alpha(\mathbf{r}_1)\ . \tag{B6}$$

As a technical point, our knowledge of these diagrams is limited to when $\mathbf{r}_1$ is well inside the sample. It is outside the scope of our theory to know what happens within a mean free path of the boundary. We can circumvent this difficulty by simply defining $\Gamma_\alpha(\mathbf{r}_1)$ such that

$$C_\alpha(\mathbf{r}_1)=\int d\mathbf{r}_1'\nabla_{1\alpha}\bar{d}(\mathbf{r}_1,\mathbf{r}_1')\Lambda(\mathbf{r}_1')+\bar{\Gamma}_\alpha(\mathbf{r}_1')\ , \tag{B7}$$

where now $-\nabla^2\bar{d}=\delta$ (a true Dirac δ function) even near the boundary. Clearly, in the middle of the sample $\Gamma_\alpha=\Gamma_\alpha$, while near the edge it may be different. Note that the boundary condition satisfied by d and the fact that $C_n(\mathbf{r}_1)=0$ on an insulating boundary imply that $\Gamma_n(\mathbf{r}_1)=0$ on an insulating boundary.

We are now in the position to exploit current conservation. From the divergenceless condition of $C_\alpha(\mathbf{r}_1)$, it follows that

$$\Lambda(\mathbf{r}_1)=\nabla_\alpha\bar{\Gamma}_\alpha(\mathbf{r}_1)\ . \tag{B8}$$

We can insert this into (B7) and integrate by parts. The boundary term vanishes on both metallic and insulating boundaries, so we can write

$$\begin{aligned}C_\alpha(\mathbf{r}_1)&=\int d\mathbf{r}_1'[\delta_{\alpha\alpha'}\delta(\mathbf{r}_1-\mathbf{r}_1')-\nabla_\alpha\nabla_{\alpha'}'d(\mathbf{r}_1,\mathbf{r}_1')]\Gamma_{\alpha'}(\mathbf{r}_1')\\&=\int d\mathbf{r}_1'\phi_{\alpha\alpha'}(\mathbf{r}_1,\mathbf{r}_1')\Gamma_{\alpha'}(\mathbf{r}_1')\ .\end{aligned} \tag{B9}$$

Since Γ differs from Γ only in the thin region on the boundary, we can effectively replace Γ by Γ. We can also repeat this process on the other variables. The end result is

$$C_{\alpha\beta\gamma\delta}(\mathbf{r}_1,\mathbf{r}_2;\mathbf{r}_3,\mathbf{r}_4)=\int\int\int\int d\mathbf{r}_1'd\mathbf{r}_2'd\mathbf{r}_3'd\mathbf{r}_4'\phi_{\alpha\alpha'}(\mathbf{r}_1,\mathbf{r}_1')\phi_{\beta\beta'}(\mathbf{r}_2,\mathbf{r}_2')\phi_{\gamma\gamma'}(\mathbf{r}_3,\mathbf{r}_3')\phi_{\delta\delta'}(\mathbf{r}_4,\mathbf{r}_4')\Gamma_{\alpha'\beta'\gamma'\delta'}(\mathbf{r}_1',\mathbf{r}_2';\mathbf{r}_3',\mathbf{r}_4')\ , \tag{B10}$$

where Γ is calculated by evaluating the diagrams in Fig. 2 in real space.

APPENDIX C

We now show that when one integrates over cross sections, one need only consider diagrams which include a change in the sign of the energy at the current vertex. Alt'shuler *et al.*[3] have suggested an argument based on momentum-space calculations. Here we do it in real space. To do this we write the conductivity as a sum of four terms obtained by multiplying out Eq. (1),

$$\sigma_{\alpha\beta}(\mathbf{r},\mathbf{r}')=\sigma_{\alpha\beta}^{+-}+\sigma_{\alpha\beta}^{-+}-\sigma_{\alpha\beta}^{++}-\sigma_{\alpha\beta}^{--} , \tag{C1}$$

where

$$\sigma_{\alpha\beta}^{\pm\pm}(\mathbf{r},\mathbf{r}')=(e^2/m^2)\pi G^{\pm}(\mathbf{r},\mathbf{r}')\overleftrightarrow{\nabla}_{\alpha}\overleftrightarrow{\nabla}_{\beta}G^{\pm}(\mathbf{r}',\mathbf{r}) . \tag{C2}$$

Consider σ^{++}, which has the property

$$\nabla_{\alpha}\sigma_{\alpha\beta}^{++}(\mathbf{r},\mathbf{r}') =2\pi(e^2/m)\delta(\mathbf{r}-\mathbf{r}')\nabla_{\beta}[G^{+}(\mathbf{r},\mathbf{r}')+G^{+}(\mathbf{r}',\mathbf{r})] . \tag{C3}$$

That is, it is divergenceless except at $\mathbf{r}=\mathbf{r}'$. If we integrate over cross sections and define

$$\bar{\sigma}^{++}(z,z')=\int\int d\mathbf{S}_{\alpha}d\mathbf{S}'_{\beta}\sigma_{\alpha\beta}^{++}(\mathbf{S},z,\mathbf{S}',z') , \tag{C4}$$

then, unless $z=z'$, $\bar{\sigma}^{++}(z,z')$ must be just a constant. Thus it can be evaluated outside of the disordered region, where the electron states are simple plane waves and σ^{++} can trivially be shown to be zero. This means that $\bar{\sigma}$ must be proportional to $\delta(z,z')$. The weight can be found by integrating $\nabla_z\sigma^{++}(z,z')$ multiplied by $z-z'$. Upon doing this integral by parts, one finds

$$\sigma^{++}(z,z')=4\pi(e^2/m)\delta(z-z')\int d\mathbf{S}_z d\mathbf{S}'_z G^{+}(z\mathbf{S},z'\mathbf{S}') . \tag{C5}$$

Thus, σ^{++} can be expressed in terms of a single-electron Green's function which is diagrammatically represented by a single line. One can then construct diagrams to calculate $\langle\sigma^{++}(z_1,z_2)\sigma(z_3,z_4)\rangle$ by drawing a conductivity bubble and a single Green's-function line connected in all possible ways by impurity lines. If one evaluates these diagrams, one finds that they are all zero in our approximation, since they are higher order in the disorder parameter $1/k_F l$ than the terms we are keeping. Thus, when calculating $C_{\alpha\beta\gamma\delta}(\mathbf{r}_1,\mathbf{r}_2;\mathbf{r}_3,\mathbf{r}_4)$ integrated over cross sections, we need only consider diagrams in which the sign of the energy changes at the current vertices. There are three such diagrams as shown in Fig. 3. This corroborates the result quoted by Alt'shuler *et al.*,[3] which, strictly speaking, was valid only in an infinite homogeneous system.

APPENDIX D

In this section we calculate the correlations in the magnetic field generated by the currents flowing through the sample. That is, we calculate $\langle\mathbf{B}(\mathbf{r}_1)\cdot\mathbf{B}(\mathbf{r}_2)\rangle$. We consider a translationally invariant system in three dimensions. The magnetic field can be calculated from the Biot-Savart law:

$$B(\mathbf{r}_1)=\frac{1}{c}\int d\mathbf{r}\frac{(\mathbf{r}-\mathbf{r}_1)\times\mathbf{j}(\mathbf{r})}{|\mathbf{r}-\mathbf{r}_1|^3} . \tag{D1}$$

We can express the fluctuations as

$$\langle B_{\mu}(\mathbf{r}_1)B_{\mu}(\mathbf{r}_2)\rangle=\frac{1}{c^2}\int\int d\mathbf{r}d\mathbf{r}'\varepsilon_{\mu\alpha\beta}\varepsilon_{\mu\gamma\delta}\frac{(r-r_1)_{\alpha}(r'-r_2)_{\gamma}}{|\mathbf{r}-\mathbf{r}_1|^3|\mathbf{r}'-\mathbf{r}_2|^3}\langle j_{\beta}(\mathbf{r})j_{\delta}(\mathbf{r}')\rangle , \tag{D2}$$

where we have expressed the cross products in terms of the Levi-Cività symbol. If we define $\mathbf{R}=\mathbf{r}_1-\mathbf{r}_2$ and use translational invariance, we can use Eq. (5.7) to write this as

$$E^2L\left[\frac{e^2}{hc}\right]^2\int\int d\mathbf{x}\,d\mathbf{y}(\delta_{\alpha\gamma}\delta_{\beta\delta}-\delta_{\alpha\delta}\delta_{\beta\gamma})\frac{x_{\alpha}y_{\gamma}}{|\mathbf{x}|^3|\mathbf{y}|^3}\phi_{\beta\delta}(\mathbf{x}-\mathbf{y}+\mathbf{R}) . \tag{D3}$$

There will be contributions from the short- and long-range parts of $\phi_{\beta\delta}$. The contribution from the short-range part is

$$E^2L\left[\frac{e^2}{hc}\right]^2\int\int d\mathbf{x}\,d\mathbf{y}\,2\frac{x_{\alpha}y_{\alpha}}{|\mathbf{x}|^3|\mathbf{y}|^3}\delta(\mathbf{x}-\mathbf{y}+\mathbf{R})=E^2L\left[\frac{e^2}{hc}\right]^2\int d\mathbf{x}\,2\frac{x_{\alpha}(x_{\alpha}+R_{\alpha})}{|\mathbf{x}|^3|\mathbf{x}+\mathbf{R}|^3} . \tag{D4}$$

If one calculates the contribution due to the long-range part of the current-current correlation function, the result is exactly the same. That is, aside from constants of order unity, the long-range nature of the current-current correlations has no effect on the magnetic field correlations. This is because the magnetic field at a given point depends nonlocally on the currents. We can extract the dependence of $|\mathbf{R}|$ by making the integral dimensionless, and we end up with a contribution

$$\langle B_{\mu}(\mathbf{r}_1)B_{\mu}(\mathbf{r}_2)\rangle\propto E^2\left[\frac{e^2}{hc}\right]^2\frac{L}{|\mathbf{R}|} . \tag{D5}$$

This expression should be cut off by the mean free path when R is small,

$$\langle B(\mathbf{r})^2\rangle\propto E^2\left[\frac{e^2}{hc}\right]^2\frac{L}{l} . \tag{D6}$$

Aronov *et al.*[8] obtained the same result by calculating fluctuations in the magnetic moment density, which is related to the magnetic field calculated here by $B(\mathbf{r})=4\pi M(\mathbf{r})$. In addition, we can calculate fluctuations in the total magnetic moment of a sample by integrating (D5) over $\mathbf{r}_1$ and $\mathbf{r}_2$. We find that

$$\left\langle \left[\int d\mathbf{r}\, M(\mathbf{r}) \right]^2 \right\rangle \propto L^6 E^2 (e^2/hc)^2 . \tag{D7}$$

Thus, the fluctuation in the average magnetic moment density (or the average magnetic field) is independent of the size of the sample.

[1]C. P. Umbach, S. Washburn, R. B. Laibowitz, and R. A. Webb, Phys. Rev. B **30**, 4049 (1984); R. A. Webb, S. Washburn, C. P. Umbach, and R. B. Laibowitz, Phys. Rev. Lett. **54**, 2696 (1985); S. Washburn, C. P. Umbach, R. B. Laibowitz, and R. A. Webb, Phys. Rev. B **32**, 4678 (1985).

[2]P. A. Lee and A. D. Stone, Phys. Rev. Lett. **55**, 1622 (1985); P. A. Lee, A. D. Stone and H. Fukuyama, Phys. Rev. B **32**, 1039 (1986).

[3]B. L. Alt'shuler and B. I. Shklovskii, Zh. Eksp. Teor. Fiz. **91**, 220 (1986) [Sov. Phys.—JETP **64**, 127 (1986)].

[4]W. J. Skocpol, P. M. Mankiewich, R. E. Howard, L. D. Jackel, D. M. Tennant, and A. D. Stone, Phys. Rev. Lett. **58**, 2347 (1987); A. Benoit, C. P. Umbach, R. B. Laibowitz, and R. A. Webb, *ibid.* **58**, 2343 (1987).

[5]R. A. Serota, S. Feng, C. L. Kane, and P. A. Lee, Phys. Rev. B **36**, 5033 (1987).

[6]C. L. Kane, P. A. Lee, and D. DiVincenzo (unpublished).

[7]S. Feng, C. L. Kane, P. A. Lee, and A. D. Stone (unpublished).

[8]A. G. Aronov, A. Yu. Zyuzin, and B. Z. Spivak, Pis'ma Zh. Theor. Fiz. **43**, 431 (1986) [JETP Lett. **43**, 555 (1986)].

[9]Daniel S. Fisher and P. A. Lee, Phys. Rev. B **23**, 6851 (1981).

[10]S. Hikami, Phys. Rev. B **24**, 2671 (1981).